Research on Anode Effect Prediction and Pretreatment in the Industrial Aluminium Electrolysis Cell Based on Zone Anode Current

Yi Meng [1], Puming Chen[2], Hao Xiao[3], Long Deng[4] and Dongwei Liu[5]
1. Associate Professor
North China University of Technology, Beijing, China
2. Senior Engineer
4. Process Engineer
Chongqing Qineng Electricity & Aluminum, Chongqing, China
3, 5. Process Engineers
Beijing SWT Intelligent Optics Technology, Beijing, China
Corresponding author: mengyi@ncut.edu.cn
https://doi.org/10.71659/icsoba2025-al050

Abstract

The increasing length of aluminium electrolysis cells has increased the probability of anode effect occurrence, and traditional anode effect detection methods and killing ways are no longer able to meet the requirements of green production of electrolytic aluminium. At present, there exists a significant delay in the judgment of the anode effect, which leads to the emission of PFC (perfluorocarbons) greenhouse gas for a certain period of time before the anode effect begins to be killed. The precise measurement technology of zone current designed by our team was used to obtain the curves of zone current vs. time in this article. It was found that there would be a certain zone where the anode current first decreased before the anode effect presented in the entire cell (or called high-voltage anode effect, HVAE), providing the possibility for early prediction of the anode effect. Further experiments had revealed that HVAE could be successfully weakened by means of adding alumina manually into the zone where its zone current decreased firstly.

Keywords: Aluminium electrolysis cell, LVAE, HVAE, Zone anode current.

1. Introduction

The anode effect (AE) occurring in aluminium reduction cells disturbs the cell operation and is harmful to the environment, since the perfluorocarbons (PFC, mainly CF_4 and C_2F_6), as extremely potent greenhouse gases, are evolved. When the concentration of locally dissolved alumina in the aluminium reduction cell is insufficient or the local current density of the anode increases to its critical current density, AE begins on several separate anodes locally and finally spreads to the whole cell [1]. AE present in one or two local anodes can be called local anode effect or low-voltage anode effect (LVAE) [2]. When the critical current density is exceeded, AE will occur on other anodes and spread in the electrolytic cell, leading to the global anode effect (or called high-voltage anode effect, HVAE) [3, 4]. With the development of large-scale aluminium reduction cells in China, the problem of uneven distribution of dissolved alumina gradually appears in aluminium reduction cells [5], so an increase in low alumina concentration areas causes an increase in the frequency of the AE coefficient.

Some methods, such as the flow-adapted alumina feeding pattern [6], the LVAE detection model [7], and the electricity-based imaging of the alumina distribution [8], have been developed to improve the uniformity of alumina concentration and to reduce the AE coefficient by controlling the feeders individually. However, it depends to the availability of accurate anode current value which can indicate the local alumina concentration. The main methods to measure the anode current are on the basis of voltage drop at different positions on the conductor [9–11], Hall sensors measurement technology [12–15] and fibre-optic current sensing (FOCS) measurement technology [16, 21]. Since FOCS can eliminate the influence of background magnetic fields totally and obtain accurate current data [17–19], it has now replaced traditional Hall sensors as the primary method for measuring the line current of aluminium reduction cells [20].

Owing to the high cost of FOCS, it was difficult to use the FOCS for online measurement of anode current in aluminium reduction cells before 2023. Luckily, a method to measure zone anode current on-line by using 5 fibre-optic loops was proposed firstly in 2023 [22, 23], and it has become economically acceptable for aluminium electrolytic plant. As a result, it is possible to predict the occurrence of AE according to the characteristics of zone current changing obtained by using this method.

This paper reports the measurement results carried out by our team on a 400 kA electrolytic cell by using a 5 fibre-optic loops measurement scheme. The characteristics of zone current changing before and after the onset of HVAE are discussed. Then both the method of HVAE prediction and the method to weaken HVAE are proposed.

2. Experimental Methods

2.1 Measurement Method of Zone Currents

The measurement experiments were conducted on a 400 kA-electrolytic cell, which had 6 feeding points evenly distributed over the space. So, this cell can be divided into 6 zones according to the feeding point, as shown in Figure 1 (a). Each zone contains four anode rods on the A side and four on the B side. Figure 1 (b) shows 5 fibre optic loops measurement scheme [22, 23]. Six fibre optic loop sensors was installed on the riser buses of the 400 kA electrolytic cell for online measurement of riser bus currents (IR1 – IR6), respectively, and sensors for measuring currents in two feeding zones (Ia1 – Ia5, Ib1 – Ib5) were installed on the anode beams of both the A side and B side simultaneously as shown in Figure 1 (a). Figure 1 (c) presents the online zone current data displayed on the industrial computer.

2.2 Feeding Reduction Experiment for Single-Zone to Produce Artificial HVAE

The feeding method for this 400 kA electrolysis cell is that, Zone 1, Zone 3 and Zone 5 are fed simultaneously, and then Zone 2, Zone 4 and Zone 6 are fed simultaneously as well. So, both the odd number zones and the even number zones are fed by means of the alternate feeding patterns, as shown in Figure 2 (a), in which a vertical line represents one feeding operation for the corresponding zone.

The feeding reduction experiment for designated single-zone was designed to produce artificial HVAE. Taking the feeding reduction experiment of Zone 1 located on tap end shown in Figure 1 (a) as an example, the feeding amount of Zone 1 was set to 0 firstly. Then the feeding mode of Zone 1 can be carried out by following the automatic feeding mode of Zone 3 and Zone 5. It means Zone 1 can be fed manually by using the manual feeding function on the control machine of electrolysis cell once both Zone 3 and Zone 5 are fed automatically. The advantage of this manual feeding method is that, the feeding mode of Zone 1 always keeps pace with the automatic feeding mode of Zones 3 and 5, no matter whether the whole feeding mode of this aluminium electrolysis cell is on the process of under feeding (UF) or over feeding (OF). Finally, if Zone 1 needs to be stopped feeding, it can be carried out by skipping manual feeding mode of Zone 1 after both Zone 3 and Zone 5 are fed automatically. Therefore, the feeding records of different zones during the feeding reduction experiment of Zone 1 were shown in Figure 2 (b), which illustrates the feeding records of Zone 1 by manual feeding mode and those of both even zones (Zone 2, Zone 4 and Zone 6) and remaining odd number zones (Zone 3 and Zone 5) carried out by automatic feeding mode. In order to produce artificial AE, the manual feeding mode of Zone

1 was set as a cycle of stopping feeding twice and then feeding once as shown in Figure 2 (b), compared to feeding records of Zone 3 and Zone 5.

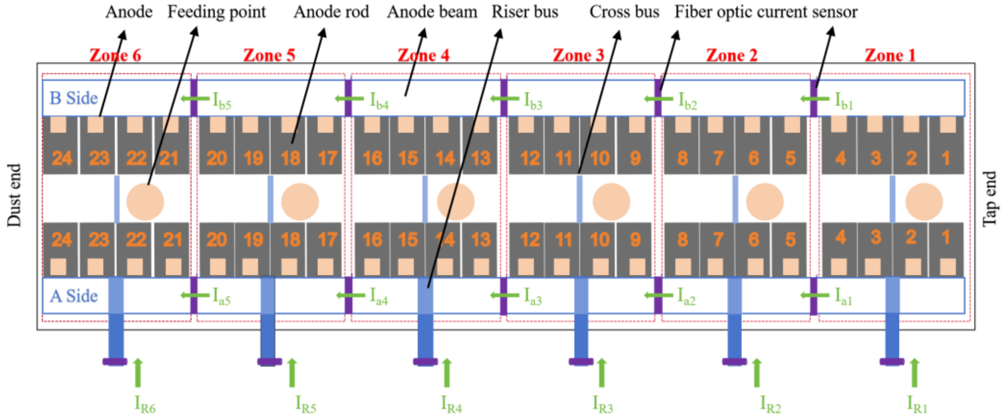

(a)

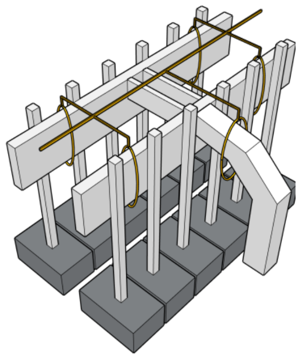

(b) (c)

Figure 1. Partition diagram of 400 kA aluminium electrolysis cell with 16 fiber optic loop sensors installation in total (a); The measurement scheme of 5 fibre optic loops installed on one zone of the cell (b) [23]; Interface of online zone current data on the computer (c).

The purpose to produce HVAE artificially is to study the effect of the manual feeding to the specific zone on HVAE weakening according to the changes of zone current before and after occurrence of HVAE. Therefore, once the zone current variation in a zone reaches to the threshold, manual feeding for this zone will be carried out as described above.

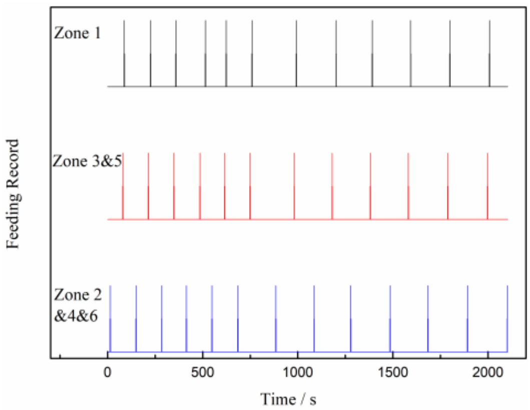

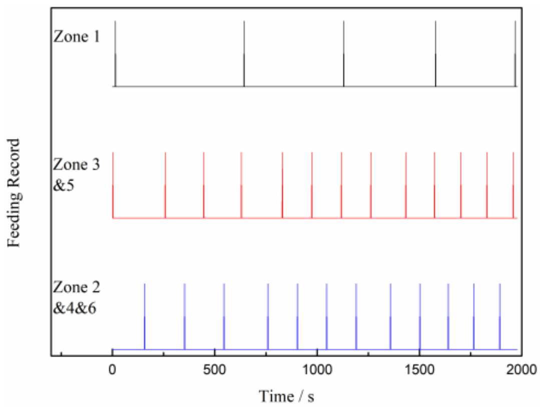

(a) (b)

Figure 2. Feeding records of different zones during the normal production of aluminium (a) and during the feeding reduction experiment of Zone 1 (b).

3. Results and Discussion

3.1 Response of Zone Current Before and After the Occurrence of HVAE

Figure 3 shows the dependence of zone current on time in 6 zones during the occurrence of the HVAE. It can be seen from Figure 3 that there is a significant fluctuation in the zone current in each zone with the maximum zone current rising to about 220 kA, far higher than the theoretical average value of zone current (~ 67 kA), while the minimum zone current decreasing to nearly 0 kA in the process of HVAE. Further, it can also be found from Figure 3 that the zone current of Zone 6 drops firstly before HVAE arriving as shown on the left side of the dashed line in Figure 3. And then the zone current of Zone 5 starts to decrease as well later, which can be considered as the spreading characteristics. The changes of the zone current curves on time in Figure 3 are similar to those reported in Reference [23]. There is no doubt that the premature decrease in zone current provides the possibility for predicting HVAE.

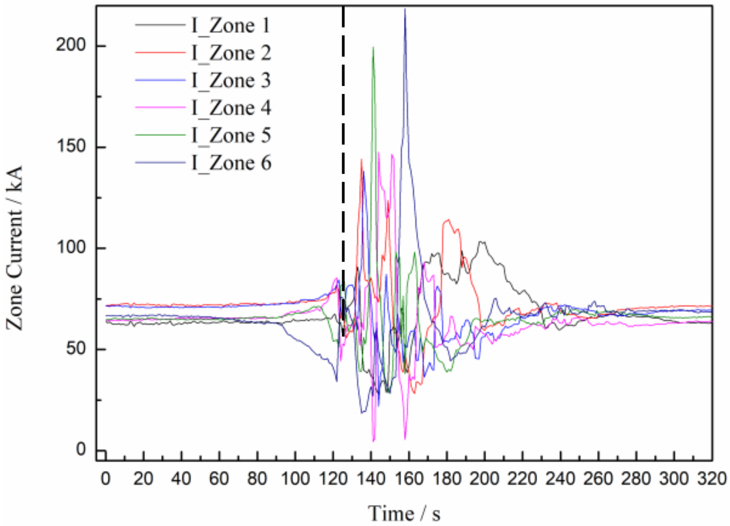

Figure 3. Dependence of zone currents of 6 zones during the occurrence of HVAE.

In order to analyse the change characteristics of the zone current in Zone 6 and its corresponding relationship with the bath voltage more clearly before the occurrence of HVAE (the curves on the left side of the dashed line shown in Figure 3), Figure 4 (a) shows the time variation curves of both the zone current in zone 6 and the bath voltage. It can be found from Figure 4 (a) that both the zone current of Zone 6 and the bath voltage vs. time are stable during 0–50 s (dashed line A), but zone current change in Zone 6 is larger than the change in bath voltage during 50–90 s (the time between dashed lines A and B). The bath voltage, which is considered as the main signal to judge the occurrence of AE for the control logic of the aluminium electrolysis cell, only starts to rise significantly after 90 s, so it can be proved that the prediction of HVAE based on zone current changing is earlier than the prediction on the basis of the bath voltage changing. Besides, the change characteristic of zone current is more obvious (Figure 4 (c)), compared to that of bath voltage shown in Figure 4 (b). Figs 4 (b) and (c) are the dependence of the bath voltage and zone current of Zone 6 on time at the time of 50–90 s (between the dashed line A and B) in Figure 4 (a), respectively. It can be discovered that the linear change characteristic of zone current with time is more obvious than that of bath voltage with time. Their determination coefficient (R2) of linear fitting is 0.94 for the zone current and 0.62 for the bath voltage, respectively, which means that the variation of the zone current has a better linear characteristic at this moment. So, it might be easier and earlier to predict HVAE on the basis of zone current changing than that based on the change of bath voltage.

3.2 HVAE Weakened by Feeding to Specific Area Based on Zone Current Response

It was thought that the HVAE might be weakened by feeding alumina to some zones once HVAE is predicted by the variation characteristics of zone current, so the feeding reduction experiment was performed to produce artificial HVAE firstly.

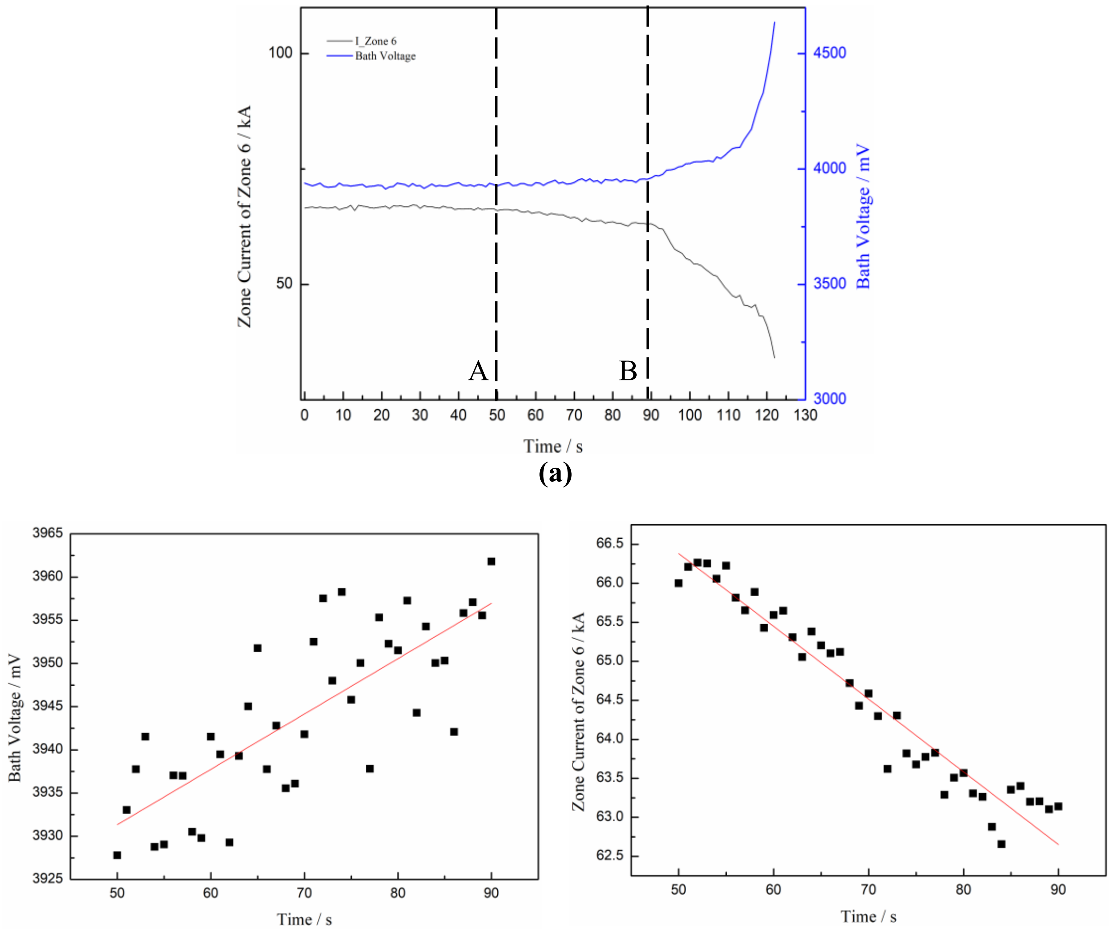

(b) (c)

Figure 4. Dependence of the zone current of Zone 6 and the bath voltage on time (a); The bath voltage *vs.* time between the dashed line A and B in (a) figure (b); Zone current of Zone 6 *vs.* time between the dashed line A and B in (a) figure (c).

After conducting the feeding reduction experiment on Zone 1 by using the feeding mode shown in Figure 2 (b), an artificial HVAE occurred approximately half an hour later. Figure 5 shows the dependence of zone current on time in 6 zones during the occurrence of the artificial HVAE. It can be seen from Figure 5 that there is a significant fluctuation in the zone current in each zone with the maximum zone current rising to over 200 kA, also far higher than the theoretical average value of zone current (~ 67 kA), and the minimum zone current decreasing to lower than 5 kA in the process of the artificial HVAE. The changes of the zone current curves in Figure 5 are similar to those in Figure 3, so it is no doubt that the change characteristics of zone currents are the same no matter whether HVAE is formed naturally or artificially. Further, it can also be found from Figure 5 that the zone current of Zone 1 (designated by arrow A in Figure 5) drops firstly before HVAE arriving as shown on the left side of the dashed line in Figure 5, which can be considered as the sign of HVAE arrival.

Figure 6 (a) shows an enlarged view of the variation curve of the zone current of Zone 1 with time in the period of 100–400 s as shown in Figure 5 and the feeding records of Zone 1, Zone 3 (representing the odd number zones other than Zone 1) and Zone 2 (representing the even number zones). It can be seen from Figure 6 (a) that at 113 s (indicated by arrow A in Figure 6 (a)), Zone 3 and Zone 5 are fed automatically by the control logic of the cell. At this time, Zone 1 is on the condition of non-feeding as shown in Figure 2 (b), so manual feeding is not carried out for Zone 1. At 164 s (indicated by arrow B in Figure 6 (a)), Zones 2, 4 and 6 are fed automatically, and the zone current of Zone 1 begins to drop gradually. In the following 36 s, although the current of Zone 1 continues to decrease, the manual feeding for Zone 1 is not started. This is to ensure that the zone current decrease in Zone 1 is caused by HVAE rather than normal fluctuation during this period, and the manual feeding for Zone 1 is started at 201 s (indicated by arrow C in Figure 6 (a)) since the zone current of Zone 1 continues to decrease by more than 10 kA in the period of 164–200 s. Finally, the zone current of Zone 1 returns to normal after 8 feeding activations as shown in Figure 6 (a). Figure 6 (b) shows the historical curve of the bath voltage taken at the production site. The fluctuation of the bath voltage in this process of HVAE is indicated in the dashed box. It is found from Figure 6 (b) that the maximum bath voltage rises only to 4.25 V in the whole HVAE process. It illustrates that it is useful to weaken HVAE by the manual feeding to a specific zone (such as Zone 1 in this experiment), once HVAE is predicted according to the corresponding characteristics of the zone current changing, as a result of weakening the abnormal rise of the bath voltage greatly.

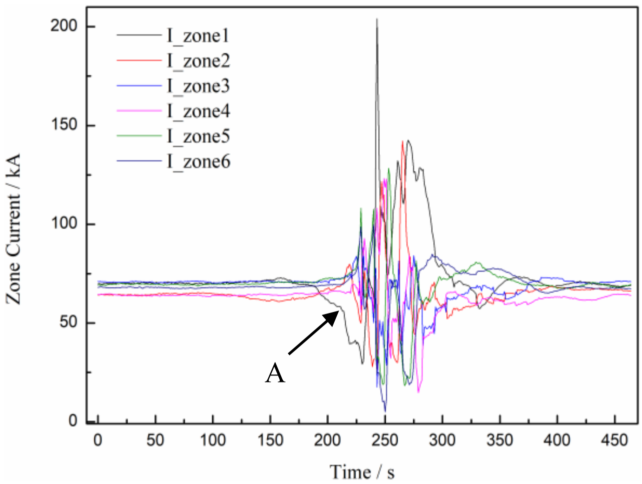

Figure 5. Dependence of zone currents of 6 zones during the artificial HVAE carried out by the feeding reduction experiment for Zone 1.

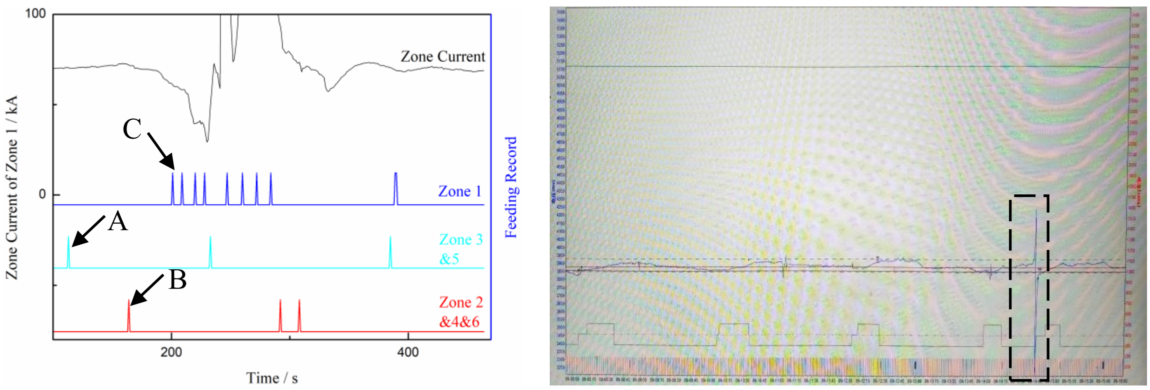

(a) (b)

Figure 6. Enlarged view of the zone current curve of Zone 1 with time period of 100–400 s in Figure 5 (a). Historical curve of the bath voltage taken at the production site (b).

4. Conclusions

In this paper, the change characteristics of zone currents with time were discussed in detail firstly, and then a feeding reduction experiment for a single zone was carried out to produce artificial HVAE. Finally, HVAE was pretreated by means of adding the alumina to the specific zones according to the characteristics of zone current changing before and after the occurrence of HVAE.

1. There is a certain zone where its zone current decreased firstly before the occurrence of HVAE. This feature makes early prediction of the anode effect possible, which is more efficient than the prediction methods carried out on the basis of the bath voltage.
2. The change of zone current for HVAE which is produced artificially by the feeding reduction experiment for single-zone is similar to that for HVAE occurring normally during production. HVAE can be weakened successfully by feeding alumina to the specific zone manually for several times according to the linear variation characteristics of zone current with time in this zone.

5. Acknowledgments

This work was financialy supported by the National Natural Science Foundation of China (No. 52 374 349).

6. References

1. Jiaqi Wang et al., Online monitoring system of alumina concentration in aluminum electrolytic cell, *Proceedings of the IEEE International Conference on Information and Automation (ICIA)*, Ningbo, China, 2016, 1–3 August 2016, 1100–1104. https://doi.org/10.1109/icinfa.2016.7831983.
2. Asbjørn Solheim, Reflections on the low-voltage anode effect in aluminium electrolysis cells, *Light Metals* 2022, 971–978.
3. Lukas Dion et al., New approach for quantification of perfluorocarbons resulting from high voltage anode effects, *Light Metals* 2018, 1469–1477. https://doi.org/10.1007/978-3-319-72284-9_192.
4. Lukas Dion et al., Simulator of non-homogenous alumina and current distribution in an aluminum electrolysis cell to predict low-voltage anode effects, *Metallurgical and Materials Transactions B* 2018, 49, 737–755. https://doi.org/10.1007/s11663-018-1174-2.
5. Jiarui Cui et al., A novel method of local anode effect prediction for large aluminum reduction cell, *Applied Sciences* 2022, 12, 12403. https://doi.org/10.3390/app122312403.
6. B. Moxnes, Asbjørn Solheim et al., Improved cell operation by redistribution of the alumina feeding, *Light Metals* 2009, 461–466.
7. Shuai Yang et al., Reducing PFCs with local anode effect detection and independently controlled feeders in aluminum reduction cells, *JOM* 2019, 72(1), 229–238. https://doi.org/10.1007/s11837-019-03786-0.
8. Joan Boulanger, Anne Gosselin, S. Gaboury et al., (2022) Imaging alumina distribution using low-voltage anode effect detections in anodic current, *Light Metals* 2022, 331–338.
9. Vinko Potocnik and Michel Reverdy, History of computer control of aluminum reduction cells, *Light Metals* 2021, 591–599. https://doi.org/10.1007/978-3-030-65396-5_81.
10. Shuai Yang et al., Online anode current signal in aluminum reduction cells: measurements and prospects, *JOM* 2016, 68(2), 623–634, https://doi.org/10.1007/s11837-015-1738-4.
11. Choon-Jie Wong, Jing Shi, Jie Bao et al., A smart individual anode current measurement system and its applications, *Light Metals* 2023, 43–51.
12. Nobuo Urata and James W. Evans, The determination of pot current distribution by measuring magnetic fields, *Light Metals* 2010, 473–478.

13. James W. Evans and Nobuo Urata, Wireless and non-contacting measurement of individual anode currents in Hall-Héroult pots; experience and benefits, *Light Metals* 2012, 939–942, https://doi.org/10.1007/978-3-319-48179-1_163.
14. Lukas Dion et al., On-line monitoring of individual anode currents to understand and improve the process control at alouette, *Light Metals* 2015, 723–728 https://doi.org/10.1002/9781119093435.ch122.
15. Lukas Dion, Charles-Luc Lagacé, François Laflamme et al., Preventive treatment of anode effects using on-line individual anode current monitoring, *Light Metals* 2017, 509–517.
16. Yongliang Wang et al., Testing and characterization of anode current in aluminum reduction cells, *Metallurgical and Materials Transactions B* 2016, 47, 1986–1998 https://doi.org/10.1007/s11663-016-0632-y.
17. Qingyu Zeng et al., Analysis of interelectrode short-circuit current in industrial copper electrorefining cells, *Measurement* 2020, 164, 108015 https://doi.org/10.1016/j.measurement.2020.108015.
18. Chun Li et al., Research of magnetic shielding on the closing gap of optical fiber current sensor, *Journal of Sensors* 2020, 2022, 3591818. https://doi.org/10.1155/2022/3591818.
19. Vinko Potocnik et al., Measurement of DC busbar currents in aluminium smelters, *Proceedings of International ICSOBA Conference*, Hamburg, 2-5 October 2017, Travaux 46, 1113-1128.
20. Klaus Bohnert et al., Fiber-optic current sensor for electrowinning of metals, *Journal of Lightwave Technology* 2007, 25(11), 3602–3609, https://doi.org/10.1109/jlt.2007.906795.
21. Yi Meng et al., Accurate measurement of anode current in aluminum electrolysis: From ideal to reality, *Light Metals* 2024, 586–595 https://doi.org/10.1007/978-3-031-50308-5_75.
22. Hao Xiao et al., A system, method and electronic equipment for measuring zone anode current in an aluminum reduction cell, *2021 China Automation Congress (CAC)* 2023. https://doi.org/10.1109/cac53003.2021.9728437.
23. Chun Li et al., Response characteristics of zone resistance in aluminium reduction cell, *Proceedings of International ICSOBA Conference*, Lyon 27-31 October 2024, *Travaux* 53, 1405-1415.